

Special Issue “Materiais 2015”

Strength and failure modes of single-*L* adhesive joints between aluminium and composites

N.R.E. Domingues^a, J.C. Trojan^b, R.D.S.G. Campilho^{a,*}, R.J.C. Carbas^b, M.D. Banea^c,
L.F.M. da Silva^b

^a*Departamento de Engenharia Mecânica, Instituto Superior de Engenharia do Porto, Instituto Politécnico do Porto, Rua Dr. António Bernardino de Almeida, 431, 4200-072 Porto, Portugal*

^b*Departamento de Engenharia Mecânica, Faculdade de Engenharia da Universidade do Porto, Rua Dr. Roberto Frias, s/n, 4200-465 Porto, Portugal*

^c*Centro Federal de Educação Tecnológica Celso Suckow da Fonseca, CEFET/RJ, Brasil*

Abstract

Adhesive bonding is a process of permanent union between the components of a structure, which is used to manufacture complex shape structures, which could not be manufactured in one piece, aiming to provide a structural joint that theoretically should be at least as resistant as the base material. Composite materials reinforced with fibres are becoming increasingly popular in many applications, as a result of a number of competitive advantages over conventional materials. Regarding the manufacture of composite structures, although the currently used techniques reduce to the maximum the connections, these are still necessary due to the typical size of the components and design, technological and logistical limitations. Moreover, it is known that in many high performance structures, it is necessary to join components in composite materials with other light metals such as aluminium, for the purpose of structural optimization. This work aims to experimentally and numerically study single-*L* adhesive joints between aluminium components and carbon-fibre reinforced composite structures under peeling loads, considering different geometric conditions and adhesives. It was found that the adhesive ductility and aluminium plate thickness are highly relevant parameters to improve the joints strength.

© 2017 Portuguese Society of Materials (SPM). Published by Elsevier España, S.L.U. All rights reserved.

Keywords: Adhesive joints; finite element method; cohesive zone models; single-*L* joints.

1. Introduction

Adhesive-bonding has grown fast in the last decades to increase the performance of structures due to its inherent advantages. During the design process of a structure that requires joining, adhesive-bonding should always be weighed against traditional techniques, due to new possibilities of lesser weight, increased stiffness and reduced costs [1]. Fibre-reinforced composite materials are becoming

increasingly popular. Composite materials are typically used in structures that require high specific strength and stiffness, which reduces the weight of components. The increasing use of composites in the aerospace industry acquired knowledge and design tools enabled expanding these materials to industries like boat building, automotive and military [2]. Although the manufacturing methods reduce to the maximum the connections, it is still necessary to join parts due to the typical size of the components and design, technological and logistical limitations [3]. Moreover, in many high performance structures, it is necessary to combine composite materials with other light metals such as aluminium or titanium, for the

* Corresponding author.

E-mail address: raulcampilho@gmail.com (R.D.S.G. Campilho)

purpose of structural optimization [4]. Joint analysis is often conducted by analytical or numerical (Finite Element, FE) methods [5]. Apart from the single-lap joint configuration, many other geometries have been studied in the literature: double-lap, butt, corner, tubular, scarf, *T*-joints and others [6].

Peel loadings have been studied for a long time [7,8]. Nase *et al.* [9] tested different adhesives in *T*-peel and fixed arm peel tests. Low-density polyethylene/isotactic polybutene-1 (iPB-1) peel films were investigated. Different amounts of iPB-1 content were tested by the *T*-peel specimen, and an exponential decrease of the strain energy release rate (G^c) was found with increasing this content. The fixed arm peel tests showed interlaminar and translaminar propagation, characterized by fracture mechanics parameters. Lin *et al.* [10] studied 180° peel tests and concluded that the peel load was dependent on the adhesive thickness (t_A) and test velocity. Zhang and Wang [11] used a Cohesive Zone Model (CZM) to model a peel test. The joints were particularly influenced by the peel rate. Applications of *T*-joints can be found in many industries such as ship building, in which bulkheads are joined to the hull [2]. Shenoi and Violette [12] addressed the effect of *T*-joint geometry under peel loadings using experimentation and numerical techniques. Single-*L* joints consist of bonding a 90° corner adherend (*L*-part) to a flat adherend. Li *et al.* [1] studied single-*L* joints under tensile and bending loads. The overlap length (L_O), t_A and *L*-part thickness (t_{P2}) played an important role on stresses. Zhang *et al.* [13] proposed a two-dimensional (2D) theoretical model to analyse peel stresses of single-*L* adhesive joints between composites and aluminium. The peeling stress distributions were a damping harmonic function with period and maximum value depending on the constituents' materials and joint geometry. FE results were compared with the proposed model, giving a good correlation.

This work aims to study, by experimentation and CZM, single-*L* adhesive joints between aluminium components and carbon-epoxy composite plates under a peel loading, considering different values of t_{P2} and adhesives of distinct ductility. The numerical analysis will enable a full understanding of the joints' behaviour, in terms of stress distributions, damage evolution, strength and failure modes. As a result, it will be possible to optimize the geometry and material parameters of the joints.

2. Experimental Part

2.1. Materials

Unidirectional carbon-epoxy pre-preg (SEAL[®] Texipreg HS 160 RM; Legnano, Italy) with 0.15 mm thickness was considered for the composite adherends of the single-*L* joints. Table 1 presents the elastic properties of a unidirectional lamina [14].

Table 1. Elastic orthotropic properties of a unidirectional carbon-epoxy ply aligned in the fibres direction (*x*-direction; *y* and *z* are the transverse and through-thickness directions, respectively) [14].

| | | |
|--------------------|------------------|-------------------|
| $E_x=1.09E+05$ MPa | $\nu_{xy}=0.342$ | $G_{xy}=4315$ MPa |
| $E_y=8819$ MPa | $\nu_{xz}=0.342$ | $G_{xz}=4315$ MPa |
| $E_z=8819$ MPa | $\nu_{yz}=0.380$ | $G_{yz}=3200$ MPa |

The aluminium adherends are made of a laminated high-strength aluminium alloy sheet (AA6082 T651). The mechanical properties of this material are available in reference [15]. The bonded joint analysis included two structural adhesives: the brittle epoxy Araldite[®] AV138 and the ductile polyurethane Sikaforce[®] 7752. Characterization of the adhesives was undertaken in previous works: E and shear modulus (G), failure strengths in tension and shear (corresponding to the CZM cohesive strengths in tension (t_n^0) and shear (t_s^0) and values of fracture toughness in tension (G_n^c) and shear (G_s^c) [5,15]. The tensile elastic and strength/strain data was obtained by bulk tests, while the relevant material properties in shear were assessed by Thick Adherend Shear Tests (TAST). The G_n^c and G_s^c values were estimated in reference [15] by inverse fitting techniques.

2.2. Joint dimensions, fabrication and testing

Fig. 1 shows the dimensions of the single-*L* joints (in mm): $L_O=25$, width $b=25$, specimen length $L_T=80$, flat adherend thickness $t_{P1}=3$, $t_{P2}=1, 2, 3$ and 4, curved element free length $L_A=60$, curved element radius $R=5$ and $t_A=0.2$. The composite plates' fabrication was undertaken by hand-lay-up followed by curing in a hot-plates press. The curved elements were bent using a manual bending machine. The bonding procedure was as follows: (1) manual abrasion of the aluminium and composite adherends at the bonding surfaces, (2) bonding in a steel mould using calibrated spacers to guarantee the selected t_A value and (3) application of pressure with grips. The joints were tensile tested in an Instron[®] 3367 testing machine, at room temperature

and constant velocity of 0.5 mm/min (Fig. 2). Each joint configuration was composed of five repetitions.

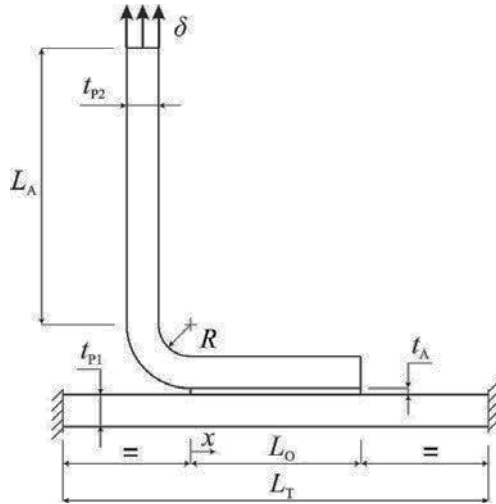


Fig. 1. Geometry of the single-L joint.

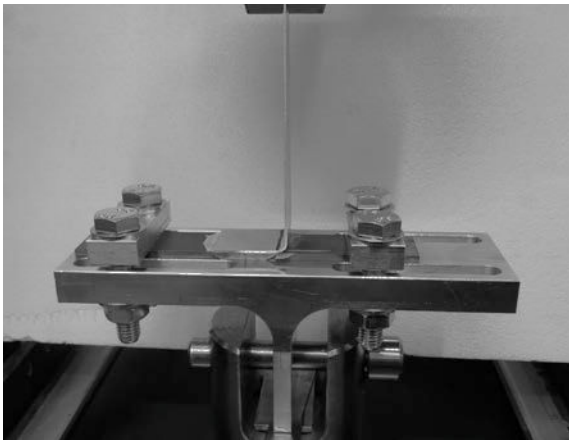


Fig. 2. Test setup for the single-L joints.

3. Numerical Part

3.1. Numerical models

A 2D geometrically non-linear static analysis was performed in Abaqus[®]. The aluminium adherends were modelled as elastic-plastic isotropic, and the CFRP adherends as elastic orthotropic, considering the data of Table 1. Different meshes were constructed for the stress and failure prediction analyses, with the former having a significantly higher refinement, to enable obtaining the stress curves with accuracy. Fig. 3 shows the details of a CZM mesh at the bonded region for $L_O=25$ mm and $t_{p2}=1$ mm. Meshes were constructed using bias effects, with smaller elements near the adhesive in the adherend thickness direction

and at the overlap edges [14,16]. The applied boundary conditions consisted of clamping the ends of the CFRP adherend and horizontally restraining the top of the curved adherend while pulling it vertically.

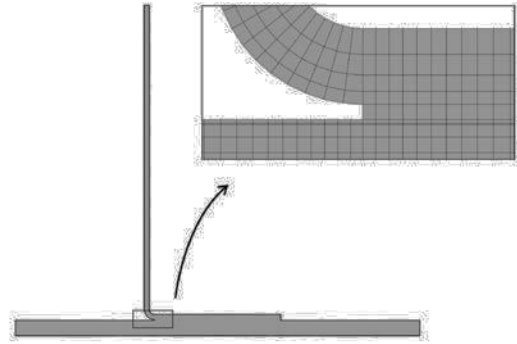


Fig. 3. Mesh detail for the CZM analysis ($t_{p2}=1$ mm).

3.2. CZM model

CZM are based on a relationship between stresses and relative displacements connecting homologous nodes of the cohesive elements (Fig. 4), to simulate the elastic behaviour up to a peak load and softening.

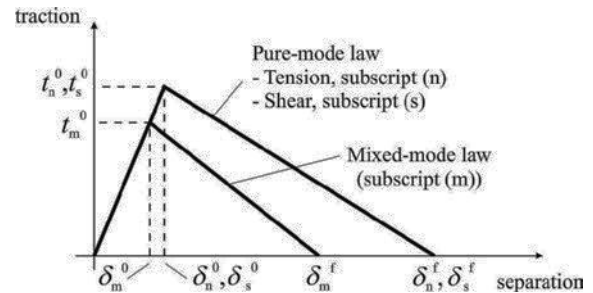


Fig. 4. Traction-separation law with linear softening law available in Abaqus[®].

The areas under the traction-separation laws in each mode of loading (tension and shear) are equalled to the respective value of G^c [17]. The traction-separation law assumes an initial linear elastic behaviour followed by linear evolution of damage.

Table 2. Cohesive parameters of the adhesives Araldite[®] AV138 and Sikaforce[®] 7752 for CZM modelling.

| Property | AV138 | 7752 |
|----------------|-------|-------|
| E (GPa) | 4.89 | 0.49 |
| G (GPa) | 1.56 | 0.19 |
| t_n^0 (MPa) | 39.45 | 11.48 |
| t_s^0 (MPa) | 30.2 | 10.17 |
| G_n^c (N/mm) | 0.20 | 2.36 |
| G_s^c (N/mm) | 0.38 | 5.41 |

Damage initiation under mixed-mode can be specified by different criteria. In this work, the quadratic nominal stress criterion was considered for the initiation of damage. Complete separation is predicted by a linear power law form of the required energies for failure in the pure modes. For full details of the presented model, see reference [15]. The cohesive parameters are summarized in Table 2.

4. Results

4.1. Peel stress distributions

Throughout this work, the longitudinal coordinate is averaged to L_0 , i.e., x/L_0 is considered (Fig. 1), with the overlap edges located at $x/L_0=0$ (at the pull-out edge) and 1 (at the farthest edge). Stresses are normalized by σ_{avg} , the average value of σ_y at the adhesive mid-thickness and $t_{p2}=1$ mm.

σ_y stresses are compared for the different values of t_{p2} and for the Araldite® AV138 and Sikaforce® 7752, respectively in Figs. 5 and 6. τ_{xy} stresses were found to be irrelevant for the joint failure. σ_y stresses peak is near $x/L_0=0$ for all t_{p2} values, although with higher normalized values for the Araldite® AV138 because of its higher stiffness. For $t_{p2}=1$ mm, over 100 times the value of σ_{avg} is reached at $x/L_0=0$.

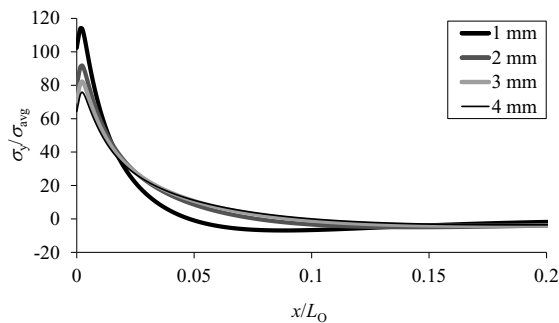


Fig. 5. σ_y stresses as a function of t_{p2} (Araldite® AV138).

This value reduces to ≈ 50 times for the Sikaforce® 7752 and $t_{p2}=1$ mm. For the Sikaforce® 7752, a much more gradual drop of σ_y stresses from the overlap edge the adhesive inner region is found, which is highly beneficial for the joint strength, especially for joints bonded with brittle adhesives, such as the Araldite® AV138 [15]. On account of this and the higher ductility of the Sikaforce® 7752, the former adhesive should have much smaller strength. With the increase of t_{p2} , the normalized σ_y peak stresses gradually diminish because of the shift in the loading type from peeling to cleavage [18]. This is more

visible for the brittle rather than the ductile adhesive. This variation implies a strength improvement of the single-L joints with the increase of t_{p2} .

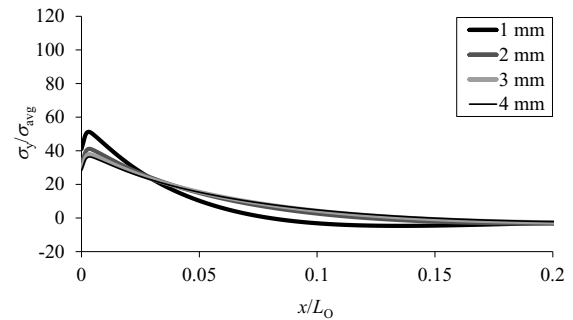


Fig. 6. σ_y stresses as a function of t_{p2} (Sikaforce® 7752).

4.2. Failure assessment

From the set of joint configurations tested in this work, only the single-L joint with $t_{p2}=1$ mm bonded with the Sikaforce® 7752 showed signs of aluminium plasticization initiating at the pull-out edge of the specimens. All failures of the single-L specimens were cohesive in the adhesive layer.

4.3. Joint strength

Figs. 7 and 8 show the experimental and numerical values of maximum load (P_m) for the single-L joints bonded with the Araldite® AV138 and Sikaforce® 7752, respectively.

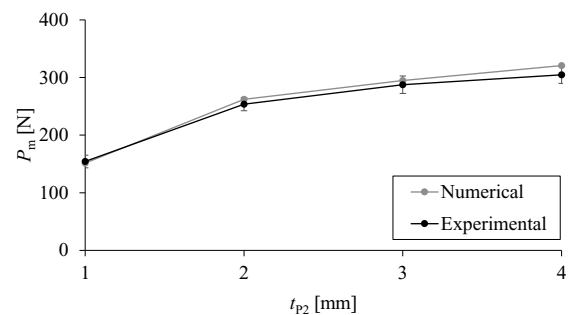


Fig. 7. P_m - t_{p2} values for the Araldite® AV138.

The results for the Araldite® AV138 show a marked P_m increase between $t_{p2}=1$ and 2 mm (64.5% improvement – experimental data), which significantly diminishes from this point on (improvement over $t_{p2}=1$ mm of 86.3% for $t_{p2}=3$ mm and 97.5% for $t_{p2}=4$ mm). By the analysis of Fig. 7 it can be concluded that the major benefit in increasing the value of t_{p2} , induced by the stiffening effect of the

L -part and consequent spreading of σ_y stresses over a larger region and reduction of σ_y peak stress, occurs between $t_{p2}=1$ and 2 mm. This adhesive is particularly affected by peak stresses because of being very stiff and brittle [15], and thus the P_m tendency closely follows the stress variations between t_{p2} values.

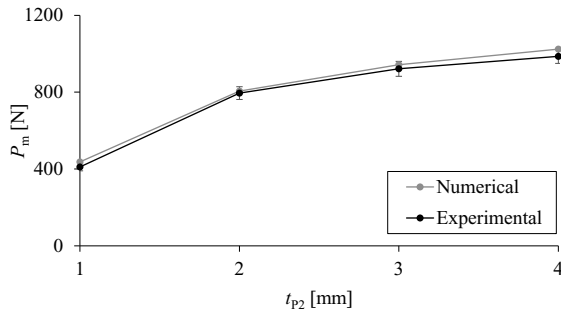


Fig. 8. P_m - t_{p2} values for the Sikaforce® 7752.

The results for the single- L joints bonded with the Sikaforce® 7752 show on first hand much higher P_m values than for those bonded with the Araldite® AV138, despite this adhesive having significantly smaller values of peel strength. However, this adhesive is much more compliant, which reflects on smaller stress gradients in the adhesive layer near to the pull-out region (Fig. 8), and it is highly ductile, which enables plasticization at the pull-out edge when its limiting strength is attained. The P_m improvement over $t_{p2}=1$ mm is 93.5% ($t_{p2}=2$ mm), 124.3% ($t_{p2}=3$ mm) and 140.1% ($t_{p2}=4$ mm).

The CZM results were consistent with the experiments for both adhesives. The maximum deviations for each adhesive, averaged over the experimental values, were of 5.3% (Araldite® AV138, single- L joint with $t_{p2}=4$ mm) and 6.25% (Sikaforce® 7752, single- L joint with $t_{p2}=1$ mm). Considering all tested configurations, these deviations were typically below 4%.

5. Conclusions

The present work aimed at studying the peeling behaviour of single- L adhesive joints between aluminium and composites. The stress analysis revealed that major σ_y peak stresses occur at $x/L_0=0$ on account of the peeling load. σ_y stresses for the Araldite® AV138 attain higher normalized peaks than

for the ductile adhesive because of the higher stiffness. By increasing t_{p2} , disregarding the adhesive type, σ_y stresses become more gradual along the bond line. This behaviour anticipated an improvement in the joint strength, but with a bigger difference between $t_{p2}=1$ and 2 mm. The experimental tests validated the numerical results. It was shown that the L -part geometry and adhesive type highly influence the joints strength. Ductile adhesives are recommended since these spread the load over a wider region, resulting in higher P_m values. Moreover, increasing t_{p2} should be considered in the design of single- L joints.

References

- [1] W. Li, L. Blunt, K.J. Stout, *Int. J. Adhes. Adhes.* 17 (1997) 303.
- [2] S.V. Nimje, S.K. Panigrahi, *Int. J. Adhes. Adhes.* 48 (2014) 139.
- [3] G. Crammond, S.W. Boyd, J.M. Dulieu-Barton, *Composites, Part A* 61 (2014) 224.
- [4] D.P. Graham, A. Rezai, D. Baker, P.A. Smith, J.F. Watts, *Composites, Part A* 64 (2014) 11.
- [5] R.D.S.G. Campilho, M.D. Banea, J.A.B.P. Neto, L.F.M. da Silva, *Int. J. Adhes. Adhes.* 44 (2013) 48.
- [6] G. Di Bella, C. Borsellino, E. Pollicino, V.F. Ruisi, *Int. J. Adhes. Adhes.* 30 (2010) 347.
- [7] D.H. Kaelble, *J. Rheol.* 3 (1959) 161.
- [8] D.H. Kaelble, *J. Rheol.* 4 (1960) 45.
- [9] M. Nase, B. Langer, W. Grellmann, *Polym. Test.* 27 (2008) 1017.
- [10] Y.Y. Lin, C.Y. Hui, Y.C. Wang, *J. Polym. Sci., Part B: Polym. Phys.* 40 (2002) 2277.
- [11] L. Zhang, J. Wang, *Int. J. Adhes. Adhes.* 29 (2009) 217.
- [12] A. Sheno, F.L.M. Violette, *J. Compos. Mater.* 24 (1990) 644.
- [13] K. Zhang, L. Li, Y. Duan, Y. Li, *Int. J. Adhes. Adhes.* 50 (2014) 37.
- [14] R.D.S.G. Campilho, M.F.S.F. de Moura, J.J.M.S. Domingues, *Compos. Sci. Technol.* 65 (2005) 1948.
- [15] R.D.S.G. Campilho, M.D. Banea, A.M.G. Pinto, L.F.M. da Silva, A.M.P. de Jesus, *Int. J. Adhes. Adhes.* 31 (2011) 363.
- [16] S.K. Panigrahi, B.J. Pradhan, *J. Reinf. Plast. Compos.* 26 (2007) 183.
- [17] M. Ridha, V.B.C. Tan, T.E. Tay, *Compos. Struct.* 93, (2010) 1239.
- [18] R.W. Messler Jr., *Joining of Materials and Structures: From Pragmatic Process to Enabling Technology*, Amsterdam: Elsevier Science B.V., 2004.